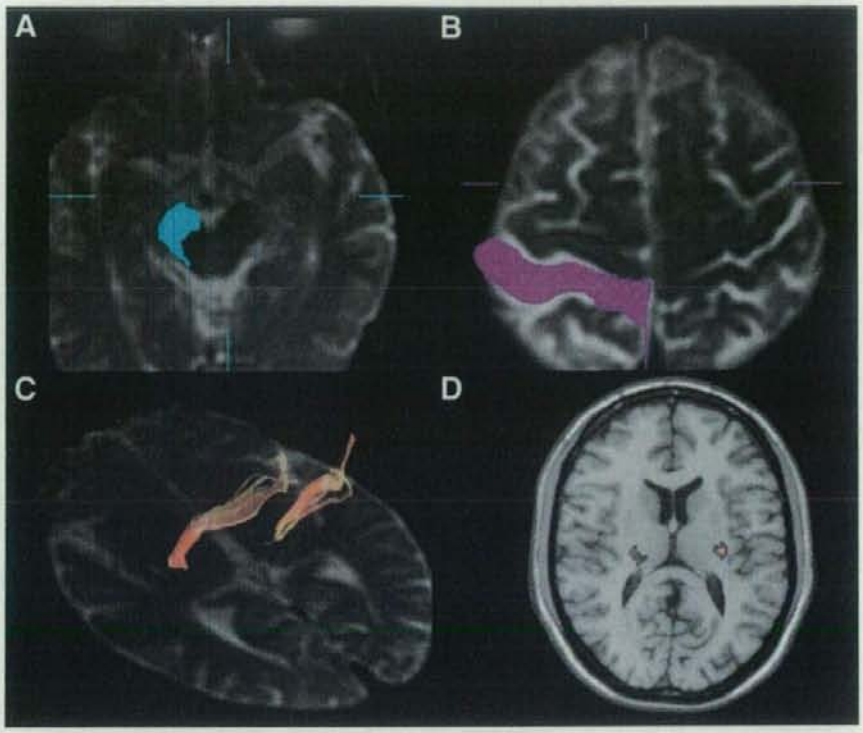

Fig. 1. Diagrams of the fiber tracking procedure. (A) The seed region of interest (ROI) is set at the cerebral peduncle, from which fiber tracking starts. (B) The target ROI is set at the precentral sulcus for the corticospinal tract (CST) and at the postcentral sulcus for the thalamocortical tract (TCT), at which fiber tracking ends. (C) Fiber tracking of the bilateral TCT on a non-diffusion-weight (b0) image. (D) Two-dimensional fiber tracking transformed to normalized space on a T1-weighted image. The number of voxels in this cross section was counted, and the ratio of the number of voxels on the affected side to the number of voxels on the unaffected side was calculated and defined as the delineation ratio.

3.3. Efficacy of rTMS and fiber tracking

The effect of rTMS of the primary motor cortex and its duration varied among the patients. For eight of the 17 patients, the VAS score after rTMS decreased by more than 30% from that before stimulation. They judged the stimulation to be effective. Eight patients indicated less than 30% reduction in the VAS score after stimulation, and only one patient reported that rTMS made the pain worse. These nine patients judged the stimulation to be ineffective.

The symptoms (level of paresis, kind of sensory abnormality, and intensity of pain) before rTMS did not affect efficacy of the stimulation. There was no significant difference in MMT scores between the rTMS-effective group and the rTMS-ineffective group, although the motor weakness tended to be mild in the rTMS-effective group (Fig. 4A). Neither was there a significant difference between groups in VAS scores before rTMS (Fig. 4B).

The rTMS-effective group had higher delineation ratio of the CST ($p = 0.02$) and the TCT ($p = 0.005$) than the rTMS-ineffective group (Fig. 4C and D). In four of the eight patients in the rTMS-ineffective group, fiber tracking of the TCT was completely impossible owing to the post-stroke lesions.

4. Discussion

The present study investigated relations between the characteristics of CPSP and the results of fiber tracking, which is the only noninvasive method of evaluating the anatomical connectivity of white matter pathways. Stroke lesions often affect the CST, the TCT, or both, causing motor weakness or sensory disturbance. Although the mechanisms of both intractable pain generation and pain reduction through rTMS remain unclear, previous studies have suggested that the mechanisms are associated with the CST and the TCT.

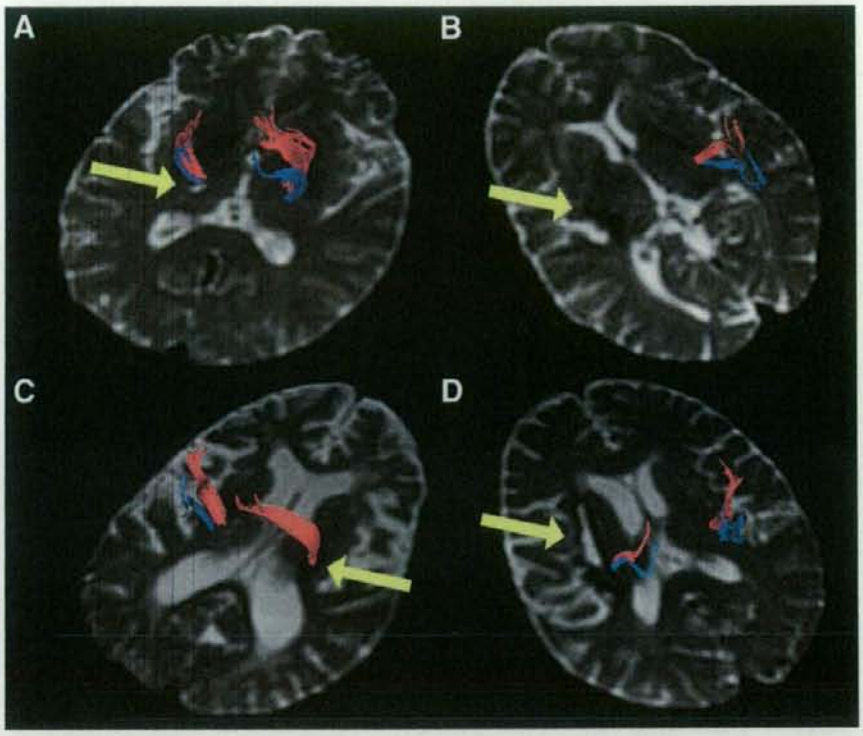

Fig. 2. Fiber tracks of the corticospinal tract (CST, red) and the thalamocortical tract (TCT, blue). b0 images are shown at the level where the CST and the TCT were impaired by post-stroke lesions (A–D). Post-stroke lesions are shown by high-intensity area (A and C) and low-intensity area (B and D) on b0 images (arrow). (A) Patient 11. The TCT is only partially delineated because of the adjacent thalamic lesion. This patient reported trunk and lower extremity pain. (B) Patient 16. The TCT terminates completely at the lesion. This patient reported pain of the entire half of the body, including the face. (C) Patient 13. The TCT is only partially delineated because of the adjacent putaminal lesion limited laterally. This patient reported lower extremity pain. (D) Patient 10. The TCT and the CST terminate completely at the lesion. This patient reported pain of the entire half of the body, including the face.

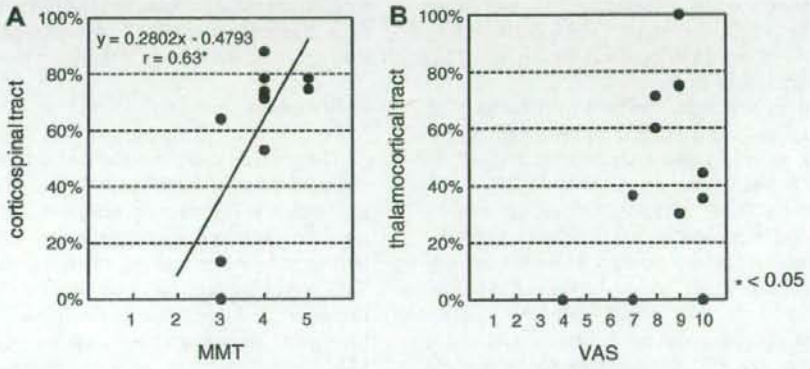

Fig. 3. Correlation between symptoms and the fiber tracking delineation ratio. (A) The manual muscle test score correlates with the delineation rate of the CST ($r = 0.63$, $p < 0.05$). (B) No correlation exists between the TCT delineation ratio and the VAS score.

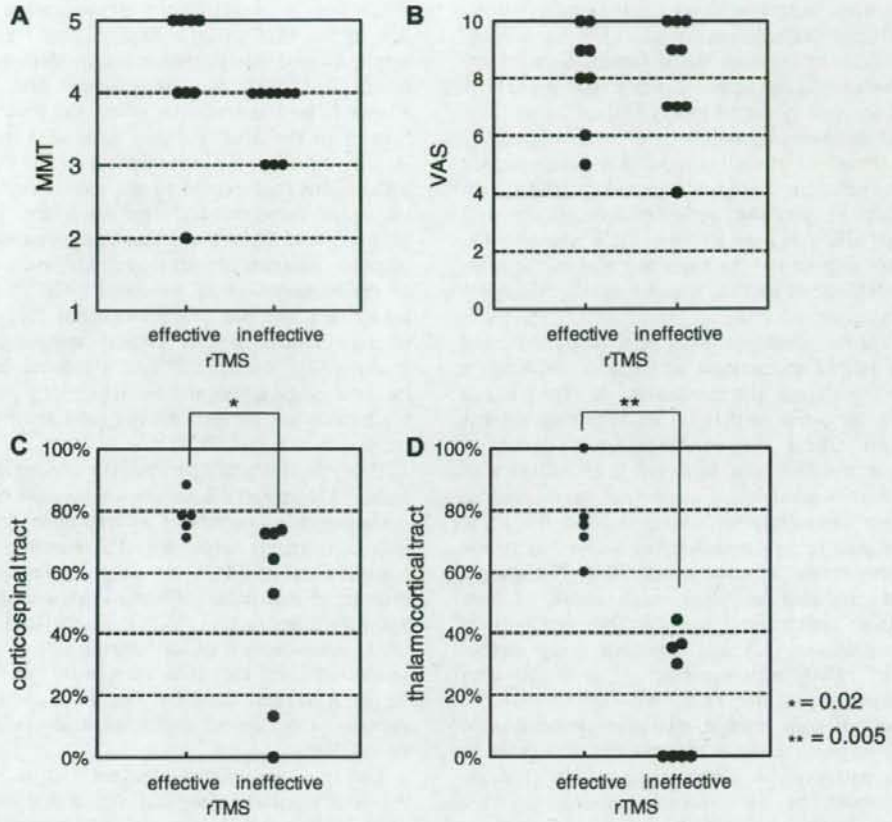

Fig. 4. Efficacy of repetitive transcranial magnetic stimulation (rTMS), pretreatment symptoms, and the fiber tracking delineation ratio. (A) No association exists between the efficacy of rTMS and the MMT score. (B) No association exists between the efficacy of rTMS and the VAS score. (C) Association between the CST delineation ratio and the efficacy of rTMS ($p = 0.02$, Mann–Whitney U test). (D) Association between the TCT delineation ratio and the efficacy of rTMS ($p = 0.005$, Mann–Whitney U test).

All our patients had a lesion impinging on the TCT. The location and size of such lesions affect the fiber tracking delineation ratio. The patients who responded to rTMS of the primary motor cortex had significantly higher CST and TCT delineation ratios than the patients who did not respond to rTMS. The TCT delineation ratio was more significantly different between rTMS-effective group and rTMS-ineffective group than the CST delineation ratio. Our results suggest that the TCT plays an important role in the mechanism of pain relief through rTMS, whereas previous studies suggested that pain control depends on an intact CST, and the relation between the efficacy of rTMS and the TCT was not emphasized.

Cerebral lesions that cause pain involve primarily the nociceptive and temperature pathways [4,5]. Microstimulation of the ventral posterior (VP) thalamus provokes pain and thermal sensations [25,29]. Craig et al. [10] suggested a different region, outside the VP, as a specific relay for pain and temperature, called the posterior portion of the ventral medial nucleus (VMpo). Anatomical and electrophysiological considerations indicate that the VP or the VMpo is the spinothalamic relay for pain and thermal sensations and that the pathway through these nuclei projects to the postcentral gyrus [3,9]. That is, a lesion of the spinothalamocortical tract is a necessary condition for CPSP [34], and in all our patients, lesions to the TCT were confirmed on three-dimensional fiber tracking images. It is proposed that spontaneous pain is linked to hyperexcitability or spontaneous discharge of thalamic or cortical neurons that have lost some of their normal input [39].

In the present study, thermal and tactile abnormalities were not quantitatively measured, and the fibers could not be delineated separately in accordance with the thalamic nuclei by the fiber tracking algorithm we

used. Therefore, comparison between the sensory disturbance and tracked fibers was not adequate. Apparently, it was difficult to evaluate the difference between Aδ fiber mediated cold and pinprick (sharpness) and C fiber mediated warmth in the periphery [13] as far as these tracked fibers were assessed.

MCS, electrical stimulation of the brain surface with grid electrodes, has been reported to relieve pain [1,14,16,24]. In positron emission tomography and functional MR imaging studies, MCS changes the activity not only of the thalamus but also of the anterior cingulate cortex and the anterior insula, which are related to emotional function [11,12]. MCS for treatment of chronic deafferentation pain modulates pain pathways related to emotion and mood, resulting in pain relief. Although the mechanism of rTMS is not necessarily the same as that of MCS, it may be that rTMS also affects the emotional pain pathways. Chronic neuropathic pain, however, is associated with motor cortex disinhibition, suggesting that impaired GABAergic neurotransmission is related to some aspects of pain or to the underlying sensory or motor disturbances caused by an impaired TCT. The analgesic effects produced by MCS could result, at least partly, from restoration of defective intracortical inhibitory processes [22]. In the present study, ineffectiveness of rTMS was significantly associated with poor delineation of the TCT. We suggest that the effectiveness of pain relief is less when delineation of the TCT is poor because modulation of signals in the pain pathway or cortex weakens, or because hyperexcitability or spontaneous discharges in thalamic or cortical neurons enlarge so as to prevent modulation as the degree of TCT impairment increases. In previous studies of MCS, the success rate tended to be lower in cases of CPSP than in cases of pain of spinal cord or peripheral origin [33]. These findings also support the idea that the existence of a lesion of the thalamocortical pathway leads to the inefficacy of rTMS.

Patients with poor delineation of the CST were likely to be unsatisfactory candidates for rTMS. Katayama et al. [17] reported that pain control following MCS tended to be unsatisfactory in patients who displayed moderate or severe motor weakness, and that the pain control afforded by MCS requires intact CST neurons originating from the motor cortex. In the present study, patients with poor delineation of the CST tended not to respond to rTMS, even though our patients did not display severe motor weakness. This result is consistent with the suggestion that intact CST neurons are required for effective pain treatment. Some correlation was also shown between the MMT score and the volume of the CST delineated by fiber tracking, which indicates that poor delineation of the CST reflects the degree of paresis as well as damage to the CST.

Yamada et al. [41] reported somatotopic organization of the TCT using a different fiber tracking algorithm. In our study, conventional MR imaging and color-coded DTI showed patients with putaminal lesions limited laterally to where the lower extremity fiber is in the fiber tracking data of Yamada et al. [41], have pain in the lower extremity, and that patients with lesions that extend to the medial portion, where the upper extremity and face fibers are, have upper extremity and facial pain. This finding shows that pain occurs in accordance with the somatotopic organization of the impaired TCT. As for the CST, although an association has been found between the position of lacunar infarctions and clinical symptoms by fiber tracking [21], we did not find a relation between the location of the lesion and the region of paresis, probably because our patients did not have severe paresis but mainly an impaired TCT.

Reproducibility of fiber tracking in normal subjects is high and asymmetry is not shown, whereas the standard deviation on a quantity of tracked fibers between subjects is relatively large [40]. The absolute volume of tracked fibers could not be compared between patients because of individual differences originating from age, sex, and other factors [35,36]. In our study, the ratio of the cross section of the affected side to that of the unaffected side, the delineation ratio, was calculated for the CST and the TCT, but we could not exclude the possibility that the stroke lesion affected the contralateral fibers.

Our study was limited by several factors. Fiber tracking is a relatively new and still developing method. Methodological issues remain, and results must be interpreted carefully. For example, it is difficult to discern white matter pathways in regions where fibers cross and branch. In such areas, the diffusion anisotropy is low, owing to the partial volume effect. Solutions to these problems can be found by applying such techniques as multiple tensor field regularization [19,37], mutual information image registration procedures [15,32], guided tensor restored anatomical connectivity tractography [7], and probabilistic fiber tracking [2]. In popular streamline tract tracing algorithms, such as the one used in this study, tracking can only progress when there is a high certainty of the fiber direction. This means it is difficult to accurately trace the pathway from a nucleus such as the thalamus, and the streamline represented may be a complex of parts of the various tracts. In addition, because fiber delineation is attenuated by the low FA value of edema, transformation by pressure from the lesion, and artifacts due to hemosiderin depositions, fiber tracking data do not always represent an actual nerve bundle [18]. Therefore, we excluded subjects with two or more stroke lesions, and the effects from the lesion were decreased because more than 6 months had passed from the onset of stroke.

In conclusion, the present study relates the characteristics of CPSP and the efficacy of rTMS to the results of fiber tracking. Previous studies suggested that pain control requires an intact CST, but the relation between the efficacy of rTMS and the TCT was not emphasized. In our study, the efficacy of rTMS was more strongly associated with lesions of the TCT than with lesions of the CST. The efficacy of rTMS for CPSP can be predicted by means of fiber tracking, and severe impairment of thalamic nuclei and the TCT may affect hyperexcitability in the thalamus and cortex or the rTMS pain relief pathway.

Conflict of interest

The authors declare no conflict of interest.

Acknowledgement

This study was supported by Ministry of Health, Labor and Welfare, Japan.

References

[1] Andre-Obadia N, Peyron R, Mertens P, Mauguiere F, Laurent B, Garcia-Larrea L. Transcranial magnetic stimulation for pain control. Double-blind study of different frequencies against placebo, and correlation with motor cortex stimulation efficacy. Clin Neurophysiol 2006;117:1536–44.

[2] Behrens TE, Johansen-Berg H, Woolrich MW, Smith SM, Wheeler-Kingshott CA, Boulby PA, et al. Non-invasive mapping of connections between human thalamus and cortex using diffusion imaging. Nat Neurosci 2003;6:750–7.

[3] Blomqvist A, Zhang ET, Craig AD. Cytoarchitectonic and immunohistochemical characterization of a specific pain and temperature relay, the posterior portion of the ventral medial nucleus, in the human thalamus. Brain 2000;123:601–19.

[4] Boivie J, Leijon G, Johansson I. Central post-stroke pain – a study of the mechanisms through analyses of the sensory abnormalities. Pain 1989;37:173–85.

[5] Bowsher D. Central pain: clinical and physiological characteristics. J Neurol Neurosurg Psychiatry 1996;61:62–9.

[6] Canavero S, Bonicalzi V, Dotta M, Vighetti S, Asteggiano G, Cocito D. Transcranial magnetic cortical stimulation relieves central pain. Stereotact Funct Neurosurg 2002;78:192–6.

[7] Cheng P, Magnotta VA, Wu D, Nopoulos P, Moser DJ, Paulsen J, et al. Evaluation of the GTRACT diffusion tensor tractography algorithm: a validation and reliability study. Neuroimage 2006;31:1075–85.

[8] Cho SH, Kim SH, Choi BY, Cho SH, Kang JH, Lee CH, et al. Motor outcome according to diffusion tensor tractography findings in the early stage of intracerebral hemorrhage. Neurosci Lett 2007;421:142–6.

[9] Craig AD, Blomqvist A. Is there a specific lamina I spinothalamocortical pathway for pain and temperature sensations in primates? J Pain 2002;3:95–101. Discussion: 113–4.

[10] Craig AD, Bushnell MC, Zhang ET, Blomqvist A. A thalamic nucleus specific for pain and temperature sensation. Nature 1994;372:770–3.

[11] Ducreux D, Attal N, Parker F, Bouhassira D. Mechanisms of central neuropathic pain: a combined psychophysical and fMRI study in syringomyelia. Brain 2006;129:963–76.

[12] Garcia-Larrea L, Peyron R, Mertens P, Gregoire MC, Lavenne F, Le Bars D, et al. Electrical stimulation of motor cortex for pain control: a combined PET-scan and electrophysiological study. Pain 1999;83:259–73.

[13] Hansson P, Backonja M, Bouhassira D. Usefulness and limitations of quantitative sensory testing: clinical and research application in neuropathic pain states. Pain 2007;129:256–9.

[14] Hirayama A, Saitoh Y, Kishima H, Shimokawa T, Oshino S, Hirata M, et al. Reduction of intractable deafferentation pain by navigation-guided repetitive transcranial magnetic stimulation of the primary motor cortex. Pain 2006;122:22–7.

[15] Horsfield MA. Mapping eddy current induced fields for the correction of diffusion-weighted echo planar images. Magn Reson Imaging 1999;17:1335–45.

[16] Johnson S, Summers J, Pridmore S. Changes to somatosensory detection and pain thresholds following high frequency repetitive TMS of the motor cortex in individuals suffering from chronic pain. Pain 2006;123:187–92.

[17] Katayama Y, Fukaya C, Yamamoto T. Poststroke pain control by chronic motor cortex stimulation: neurological characteristics predicting a favorable response. J Neurosurg 1998;89:585–91.

[18] Konishi J, Yamada K, Kizu O, Ito H, Sugimura K, Yoshikawa K, et al. MR tractography for the evaluation of functional recovery from lenticulostriate infarcts. Neurology 2005;64:108–13.

[19] Kreher BW, Schneider JF, Mader I, Martin E, Hennig J, Il'yasov KA. Multitensor approach for analysis and tracking of complex fiber configurations. Magn Reson Med 2005;54:1216–25.

[20] Kunimatsu A, Aoki S, Masutani Y, Abe O, Mori H, Ohtomo K. Three-dimensional white matter tractography by diffusion tensor imaging in ischaemic stroke involving the corticospinal tract. Neuroradiology 2003;45:532–5.

[21] Lee JS, Han MK, Kim SH, Kwon OK, Kim JH. Fiber tracking by diffusion tensor imaging in corticospinal tract stroke: topographical correlation with clinical symptoms. Neuroimage 2005;26:771–6.

[22] Lefaucheur JP, Drouot X, Menard-Lefaucheur I, Keravel Y, Nguyen JP. Motor cortex rTMS restores defective intracortical inhibition in chronic neuropathic pain. Neurology 2006;67:1568–74.

[23] Lefaucheur JP, Drouot X, Menard-Lefaucheur I, Zerah F, Bendib B, Cesaro P, et al. Neurogenic pain relief by repetitive transcranial magnetic cortical stimulation depends on the origin and the site of pain. J Neurol Neurosurg Psychiatry 2004;75:612–6.

[24] Lefaucheur JP, Hatem S, Nineb A, Menard-Lefaucheur I, Wendling S, Keravel Y, et al. Somatotopic organization of the analgesic effects of motor cortex rTMS in neuropathic pain. Neurology 2006;67:1998–2004.

[25] Lenz FA, Seike M, Richardson RT, Lin YC, Baker FH, Khoja I, et al. Thermal and pain sensations evoked by microstimulation in the area of human ventrocaudal nucleus. J Neurophysiol 1993;70:200–12.

[26] Merskey H, Lindblom U, Mumford JM, Nathan PW, Noordenbos W, Sunderland S. Pain terms: current list with definitions and notes on usage. Pain 1986:S217–21.

[27] Meyer JW, Makris N, Bates JF, Caviness VS, Kennedy DN. MRI-Based topographic parcellation of human cerebral white matter. Neuroimage 1999;9:1–17.

[28] Mori S, Crain BJ, Chacko VP, van Zijl PC. Three-dimensional tracking of axonal projections in the brain by magnetic resonance imaging. Ann Neurol 1999;45:265–9.

[29] Ohara S, Lenz FA. Medial lateral extent of thermal and pain sensations evoked by microstimulation in somatic sensory nuclei of human thalamus. J Neurophysiol 2003;90:2367–77.

[30] Parker GJ, Stephan KE, Barker GJ, Rowe JB, MacManus DG, Wheeler-Kingshott CA, et al. Initial demonstration of

in vivo tracing of axonal projections in the macaque brain and comparison with the human brain using diffusion tensor imaging and fast marching tractography. Neuroimage 2002;15: 797–809.

[31] Reich DS, Smith SA, Jones CK, Zackowski KM, van Zijl PC, Calabresi PA, et al. Quantitative characterization of the corticospinal tract at 3T. AJNR Am J Neuroradiol 2006;27:2168–78.

[32] Rohde GK, Barnett AS, Basser PJ, Marenco S, Pierpaoli C. Comprehensive approach for correction of motion and distortion in diffusion-weighted MRI. Magn Reson Med 2004;51:103–14.

[33] Saitoh Y, Hirayama A, Kishima H, Oshino S, Hirata M, Kato A, et al. Stimulation of primary motor cortex for intractable deafferentation pain. Acta Neurochir Suppl 2006;99:57–9.

[34] Seghier ML, Lazeyras F, Vuilleumier P, Schnider A, Carota A. Functional magnetic resonance imaging and diffusion tensor imaging in a case of central poststroke pain. J Pain 2005;6:208–12.

[35] Stadlbauer A, Salomonowitz E, Strunk G, Hammen T, Ganslandt O. Age-related degradation in the central nervous system: assessment with diffusion-tensor imaging and quantitative fiber tracking. Radiology 2008;247:179–88.

[36] Sullivan EV, Rohlfing T, Pfefferbaum A. Quantitative fiber tracking of lateral and interhemispheric white matter systems in normal aging: Relations to timed performance. Neurobiol Aging, in press.

[37] Tuch DS, Reese TG, Wiegell MR, Makris N, Belliveau JW, Wedeen VJ. High angular resolution diffusion imaging reveals intravoxel white matter fiber heterogeneity. Magn Reson Med 2002;48:577–82.

[38] Valeriani M, Rambaud L, Mauguiere F. Scalp topography and dipolar source modelling of potentials evoked by CO_2 laser stimulation of the hand. Electroencephalogr Clin Neurophysiol 1996;100:343–53.

[39] Vestergaard K, Nielsen J, Andersen G, Ingeman-Nielsen M, Arendt-Nielsen L, Jensen TS. Sensory abnormalities in consecutive, unselected patients with central post-stroke pain. Pain 1995;61:177–86.

[40] Wakana S, Caprihan A, Panzenboeck MM, Fallon JH, Perry M, Gollub RL, et al. Reproducibility of quantitative tractography methods applied to cerebral white matter. Neuroimage 2007; 36:630–44.

[41] Yamada K, Nagakane Y, Yoshikawa K, Kizu O, Ito H, Kubota T, et al. Somatotopic organization of thalamocortical projection fibers as assessed with MR tractography. Radiology 2007; 242:840–5.

Stroke
JOURNAL OF THE AMERICAN HEART ASSOCIATION

American Stroke Association
A Division of American Heart Association

Ipsilateral Motor-Related Hyperactivity in Patients With Cerebral Occlusive Vascular Disease

Satoru Oshino, Amami Kato, Masayuki Hirata, Haruhiko Kishima, Youichi Saitoh, Toshiyuki Fujinaka and Toshiki Yoshimine

Stroke 2008;39;2769-2775; originally published online Jul 17, 2008;
DOI: 10.1161/STROKEAHA.108.518027
Stroke is published by the American Heart Association. 7272 Greenville Avenue, Dallas, TX 72514
 Print ISSN: 0039-2499. Online ISSN: 1524-4628

Ipsilateral Motor-Related Hyperactivity in Patients With Cerebral Occlusive Vascular Disease

Satoru Oshino, MD, PhD; Amami Kato, MD, PhD; Masayuki Hirata, MD, PhD; Haruhiko Kishima, MD, PhD; Youichi Saitoh, MD, PhD; Toshiyuki Fujinaka, MD, PhD; Toshiki Yoshimine, MD, PhD

Background and Purpose—Cerebral occlusive vascular disease is an established risk factor for ischemic stroke; however, little is known about its effects on brain function in patients without stroke. To detect possible functional alterations, we used magnetoencephalography and evaluated cerebral cortical activity during hand motor tasks in a group of such patients.

Method—Event-related desynchronization (ERD) during hand-grasping and self-paced finger-tapping tasks was examined in 38 right-hand-dominant patients with occlusive disease of the internal carotid or middle cerebral artery caused by diverse pathologies (atherosclerosis, 28; others, 10) and in 8 control subjects. All patients had no apparent motor impairments. The spatial distribution and the intensity (t value) of ERD in the beta band were analyzed with synthetic aperture magnetometry. According to the laterality index calculated from the ratios of peak t values on ipsilateral vs contralateral (with respect to the hand movement) hemispheres, the distribution of ERD was classified into 3 patterns: contralateral, bilateral, and ipsilateral.

Results—Abnormal ipsilateral dominant distribution of beta ERD was observed significantly more often during contralesional hand grasping in patients with atherosclerotic vascular lesion. It was accompanied by significantly higher t values on the ipsilateral hemisphere, without a decrease in those on the contralateral side. The age, the rating scores of periventricular hyperintensity, and ventricular size were all significantly higher in patients who showed the ipsilateral-dominant pattern.

Conclusion—Abnormal ipsilateral hyperactivity may indicate the presence of subclinical functional alterations related to atherosclerotic occlusive vascular disease. **(*Stroke*. 2008;39:2769-2775.)**

Key Words: carotid stenosis ■ functional imaging ■ ischemia ■ neurophysiology

Severe stenosis, or occlusion, of the internal carotid artery (ICA) or middle cerebral artery (MCA) is an established risk factor for stroke and a target for neurosurgical procedures aimed at its prevention.[1,2] Although cerebral blood flow (CBF), metabolism, and morphological changes in this pathology have been evaluated in some detail using modern neuroimaging techniques, little is known if brain function itself is altered under such ischemic conditions, particularly when infarction is absent. It is a common observation that patients with cerebral occlusive vascular disease show no apparent neurological symptoms, even in a state of severe hypoperfusion called "misery perfusion." Nevertheless, some decline in cognition has been detected in asymptomatic as well as symptomatic patients with carotid artery stenosis,[3] which indicates that brain function can be altered even without any history of stroke. Because cognitive function reflects activity of the whole brain, it is not easy to distinguish the contributions from left and right hemispheres in cognitive tests. Hence, development of a more objective and quantitative measure could greatly help in early diagnosis and treatment of functional alteration accompanying ischemic cerebrovascular disease. The objective of this study was to evaluate subclinical alterations in motor-related brain function in patients with cerebral occlusive vascular disease who showed no apparent motor impairments.

Attenuation of the electroencephalographic power in the central brain region during hand movement or sensory stimulation was quantitatively defined as event-related desynchronization (ERD)[4,5] and thought to reflect a correlation between an activated cortical area and an increased level of neuronal excitability.[6] Because of its consistent relation to the movement, ERD in the beta band (βERD) has been considered a physiological phenomenon caused by activation of the sensorimotor cortex.[7] Moreover, it has been shown that βERD represents execution as well as programming or control of the movement.[8] In this study, we have chosen βERD as a parameter of brain

Received February 19, 2008; accepted February 26, 2008.

From Department of Neurosurgery (S.O., M.H., H.K., Y.S., T.F.,T.Y.), Osaka University Graduate School of Medicine, Osaka, Japan; Department of Neurosurgery (A.K.), Kinki University School of Medicine, Osaka, Japan.

Correspondence to Satoru Oshino, Department of Neurosurgery, Osaka University Graduate School of Medicine, 2-2 Yamadaoka, Suita, 565-0871, Osaka, Japan. E-mail s-oshino@nsurg.med.osaka-u.ac.jp

***Stroke* is available at http://stroke.ahajournals.org**

DOI: 10.1161/STROKEAHA.108.518027

function and analyzed it using magnetoencephalography (MEG) with synthetic aperture magnetometry (SAM). In particular, we were interested in the behavior of βERD during movement of the hand contralateral to the occlusive vascular lesion (contralesional hand), because such movements could activate the hemisphere of the lesion. The superior spatial resolution of MEG allows identification of the anatomic location of cortical activity with enhanced accuracy.[9] The spatial filtering technique using an adaptive beam-forming method (SAM) is a unique modality for estimating the tomographic distribution of the power or its change within a selected band frequency from MEG data.[10,11] Using SAM, the regions with significant oscillatory change are displayed on individual MR images; recently, that imaging has been clinically applied as functional neuroimaging.[9–13]

Methods

Patients

From April 2005 to June 2007, 62 adult patients with ICA/MCA stenosis, or occlusion, without ischemic stroke during the past 3 months, were admitted to the Department of Neurosurgery of Osaka University Hospital for a surgical procedure or clinical evaluation. Occlusive disease was defined as obstruction >60% according to the criteria of the North American symptomatic carotid endarterectomy trial for cervical ICA[1] and narrowing of >50% on angiography for intracranial ICA or MCA. For the current MEG study, we excluded the following categories of patients: those who showed motor symptoms or who had infarction around the motor-related regions, and those in whom large magnetic artifacts were detected in MEG recordings. After selection, 38 patients were enrolled in this study prospectively. All of them were right-hand-dominant, as determined with the Edinburgh handedness inventory,[14] and presented with no apparent motor symptoms in a routine neurological examination. In 11 patients, MRI revealed previous infarctions located in the frontal lobe (anterior to premotor cortex), occipital lobe, and in the basal ganglia, but no infarction was detected around the sensorimotor or premotor cortices, internal capsule, or corona radiata. Twenty-eight patients had atherosclerotic lesions (cervical ICA stenosis in 16, cervical ICA occlusion in 4, intracranial ICA stenosis in 2, and MCA occlusion/stenosis in 6), and the other 10 had lesions not related to atherosclerosis (intracranial ICA occlusion/stenosis attributable to moyamoya disease in 4, intracranial ICA stenosis attributable to encasement by meningioma in 1, cervical ICA occlusion attributable to Takayasu disease [occlusion from common carotid artery] in 1, occluded ICA for the treatment of tumor, giant aneurysm, and traumatic arterial dissection, respectively, in 3, and an incidental finding in 1).

Control Subjects

Eight right-hand-dominant control subjects (5 men and 3 woman), with a median age of 66 (range 55 to 79), were used as controls.

MEG Study

Motor-related magnetic field was recorded using a helmet-shaped 64-channel SQUID system (NeuroSQUID Model 100; CTF Systems Inc) in a magnetically shielded room. The patients/subjects were seated in a comfortable chair with their eyes open and were asked to stare blankly at a point in front of the chair. The MEG data were acquired with a 625-Hz sampling rate and filtered with a 200-Hz on-line low-pass filter.

After a brief explanation, the patients/subjects were asked to perform 2 kinds of hand motor tests: a hand-grasping task and a self-paced finger-tapping task. Because the latter is relatively more complex and requires greater concentration, the tasks were performed in the following order: (1) right finger tapping; (2) left finger tapping; (3) right hand grasping; and (4) left hand grasping. During performance of these tasks, subjects/patients were monitored continuously on a video camera and checked for the absence of an apparent mirror movement in the other (resting) hand. The ongoing waveform (MEG) results were displayed on a monitor and stored in the workstation memory. Each examination session was begun and terminated by measuring the head position of the patient. Before the acquisition of the actual results, 1 or 2 preliminary trials were performed to ensure that the patient performed the task correctly.

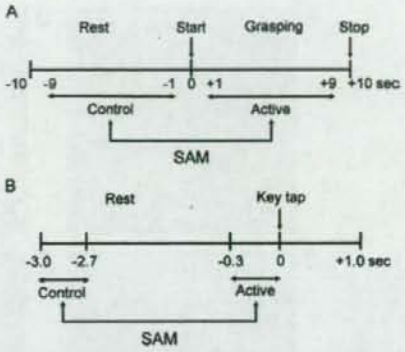

Figure 1. Data collected for a trial of the hand grasping task (A) and self-paced finger-tapping task (B). The powers of beta band between "active" and "control" time windows were statistically compared using SAM.

Task 1, the hand-grasping task (not a tonic sustained grasp), involved grasping with 1 hand weakly at a constant rate while the other hand was resting.[11,12] The working hand was supinated while the resting hand was pronated and placed on an arm rest. The data for each trial were collected relative to the trigger (sound cue or time "0") for 20 seconds and consisted of 2 periods: the "control" state in the time window −10 to 0 seconds, in which the patient remained still, and the "active" state in the time window 0 to +10 seconds, which involved grasp and release movements (Figure 1A). Six such trials, with 5-second intervals between them, were collected as an "examination," first for the right hand. Then, the positions of the hands were changed and an identical examination was performed for the left hand.

Task 2 was a self-paced index-finger-tapping test using a nonmagnetic fiber optical response keypad (LUMItouch; Photon Control Inc), which was placed on either side of the arm rest. The patients were instructed to press the keypad with their index finger, with intervals of ≈5 seconds (but without counting the time) between the taps. The data from 3 seconds before to 1 second after the key input were collected as a trial, and 60 trials were collected for each examination (Figure 1B).

Individual anatomic MR images were acquired using a 1.5-T imaging systems (Magnetom Impact; Siemens). For all measurements, fiducial skin markers were placed on the patient's nasion and at bilateral preauricular points to establish common coordinate systems for MR images and MEG.[9,11–13] This MEG protocol was approved by the ethics committee of the Osaka University Hospital. Informed consent for MEG recording was obtained from all patients and control subjects.

SAM Analysis of Motor-Related Field

Details of SAM algorithm have been described previously.[10,11] In the present study, a volumetric image of root mean squared source activity in the beta band with 5-mm voxel resolution was generated for each "control" and "active" time window: −9 to −1 and 1 to 9 seconds for task 1, and −3.0 to −2.7 and −0.3 to 0 seconds for task 2, relative to the trigger onset, respectively (Figure 1). The statistical imaging was computed subsequently by comparing the powers of the beta band (13 to 30 Hz) in both time windows on a single voxel basis over all trials using the Student t test with Jackknife statistics. The t value of each voxel was displayed in a color scale on individual MR images using the MRIViewer (CTF Systems Inc).[9] The decrease of

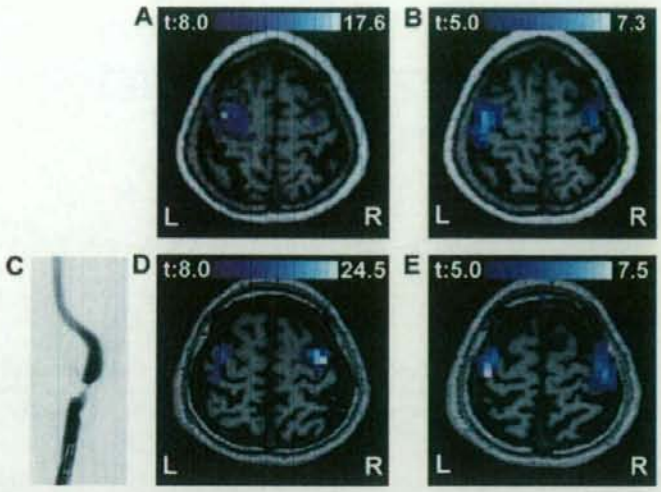

Figure 2. Voxels exhibiting statistically significant decrease in the power of β band (t value) are displayed in a blue scale. The images from a control subject (66-year-old woman) are shown as (A) (right hand grasping; Tc, 17.6; Ti, 11.3; LI, 0.22) and (B) (right finger-tapping; Tc, 7.3; Ti, 6.3; LI, 0.07). Both are classified as contralateral dominant pattern. C, The angiogram showing left carotid artery stenosis (80%) in patient 2 (65-year-old man). D, During right hand grasping in the same patient, the distribution pattern was classified as "ipsilateral-dominant" (Tc, 16.8; Ti, 24.8; LI, −0.18). E, In the same patient, a contralateral-dominant pattern (Tc, 7.5; Ti, 7.1; LI, 0.04) was seen during a right self-paced finger-tapping task.

power that indicates ERD was displayed in blue, whereas the power increase that indicates event-related synchronization (ERS) was shown in red. SAM statistical images were created for grasping and tapping tests with each hand giving 4 (2 for each task) images for each patient. Before SAM analysis, all trials were inspected visually. Data with sensors located in the most anterior or lower part of the helmet were excluded from analysis if they were accompanied by large artifacts caused by the presence of metal in the oral cavity (dental problems) or movements of eyeballs.

Patterns of Distribution of Beta Band Desynchronization

The laterality index (LI) was calculated using the peak t values around the sensorimotor area on contralateral and ipsilateral hemispheres with respect to the examined hand as follows: $LI=(Tc-Ti)/(Tc+Ti)$,[13] where Tc is the highest peak t value on the contralateral hemisphere and Ti is that on the ipsilateral hemisphere. Based on the behavior of LI, we classified the spatial distribution of βERD into 3 types: contralateral-dominant ($LI>0$), bilaterally spread ($-0.1\leq LI\leq 0$), and ipsilateral-dominant ($LI<-0.1$).

Evaluation of Sulcal Atrophy, Ventricular Size, and Periventricular White Matter Hyperintensity

The morphological changes in MR images of sulcal atrophy, ventricular size, and periventricular hyperintensity (PVH) of the hemisphere with the vascular lesion were assessed using a semiquantitative 10-point visual scale introduced by Manolio et al.[15] Three scorers, without any clinical information for patients, evaluated these 3 parameters. Sulcal atrophy and ventricular size were scored on T1-weighted images, and PVH was evaluated on FLAIR images (and not the proton images as in the original method of Manolio et al). Before analyzing the actual results, the 3 scorers performed a trial rating using MR images from a nonstudy patient and unified the scoring procedure. The variance in the visual scales among the 3 scorers was within 1 point for all parameters; hence, median values were calculated.

CBF Study With SPECT

Depending on their clinical conditions, the patients underwent [^{123}I] N-isopropyl-p-iodoamphetamine single-photon emission computed tomography (^{123}I-IMP SPECT) with or without an acetazolamide challenge test.[16] The details of SPECT procedure were reported previously.[16] Based on the neuroradiological reports, the degree of CBF impairment in the affected ICA or MCA region was categorized into 3 classes: no significant CBF reduction at rest (class A), CBF reduction at rest but with preserved vasoreactivity to acetazolamide (class B), and reduction at rest with impaired vasoreactivity (<23% increase) to acetazolamide as determined by a split-dose method (class C).[16]

Statistical Analysis

The results for age, Tc, Ti, and LI were analyzed with nonparametric Mann-Whitney U test. To compare the 2 groups of patients with respect to the presence or absence of ipsilateral dominant pattern, we used χ^2 with Fisher exact probability test. $P<0.05$ was considered as significant.

Results

Motor-Related Magnetic Fields in Control Subjects

In all control subjects, statistically determined regions of βERD with the highest t value were detected either on contralateral or ipsilateral sensorimotor, or premotor, cortex with respect to the examined hand (Figure 2A, B). The distribution patterns of βERD, peak t values (Tc and Ti), and LI during the 2 tasks are presented in Table 1. There was no evidence for the ipsilateral dominant distribution pattern of βERD, with the definition of $LI<-0.1$, in any individual in either of the tasks. Comparing the 2 tasks, the LI in hand grasping was larger than that in self-paced tapping, with an almost significant difference ($P=0.07$, Mann-Whitney U test). With respect to the side (right or left) of the examined hand, there were no significant differences in Ti, Tc, and LI

Table 1. Motor Magnetic Field Properties and βERD Distribution Patterns in Control Subjects

	Hand Grasping	Finger Tapping
Median Tc, range	13.6, 6.8–24.9	9.2, 6.0–14.2
Median Ti, range	7.5, 3.8–14.7	7.3, 3.2–11.0
Median LI, range	0.22,* −0.05–0.50	0.06, −0.05–0.38
Contralateral-dominant	15	14
Bilaterally spread	1	2
Ipsilateral-dominant	0	0

*$P=0.07$ with Mann-Whitney U test.
Results of 16 examinations (2×number of patients) are presented.

Table 2. Distribution Patterns of βERD in Patients With Vascular Occlusive Disease

Distribution Patterns	Hand Grasping	Finger Tapping
Median Tc, range	14.3, 2.8–32.3	7.6, 2.7–14.6
Median Ti , range	12.4, 5.2–25.3	6.3, 3.2–13.5
Median LI, range	0.10, −0.57–0.65	0.07, −0.19–0.37
Contralateral-dominant	53	49
Bilaterally spread	3	13
Ipsilateral-dominant	20	5

Median values (ranges) of Tc, Ti, LI, and the numbers in each distribution patterns are shown for 76 hand-grasping and 67 finger-tapping examinations.

in either tasks, although there was a slight tendency ($P=0.11$, Mann–Whitney U test) for the higher median Ti during left hand-grasping (9.7; range 6.7 to 14.3) as compared to right hand-grasping (7.4; range, 3.8 to 11.3).

Motor-Related Magnetic Fields in Patients With Occlusive Vascular Disease

In the group with atherosclerotic lesions (AS group), there were 21 men and 7 women, with an overall median age of 69 (range, 55 to 78) years; in that with nonatherosclerotic lesions (NAS group), median age was 48.5 (range, 21 to 73) and there were 4 men and 6 women. The age of the AS group was significantly higher than that of NAS ($P<0.05$, Mann-Whitney U test). According to the criteria for an "occlusive disease," 9 patients in the AS group and 4 (all with moyamoya disease) in the NAS group had bilateral lesions. The symptomatic side and, if asymptomatic, the side of the more severe stenosis or CBF reduction are listed as "the site" in supplemental Table I (available online at http://stroke.ahajournals.org). The location of a previous infarction and the presenting ischemic symptom are also given in the same Table.

All 76 hand-grasping examinations in 38 patients (ie, 1 per hand) were performed successfully. In finger-tapping, trials that contained occasional large noise or inadequate signals (eg, double taps in a trial) were eliminated. The number of excluded trials was ≈5%, with a maximum of 8 eliminated tapping trials in a single patient. However, 9 examinations of finger tapping were not available because of unforeseen problems with the measuring device in 2, injury of the relevant finger in 1, and inadequate performance attributable to sleepiness, or too-fast pacing in 6 (supplemental Table II) attributable to an unavailable cause. Therefore, 67 tapping and 76 hand-grasping examinations were analyzed.

As in control subjects, regions with the highest t values were detected around the contralateral or ipsilateral sensorimotor, or premotor, cortex (Figure 2D, E). The distribution pattern of βERD and values of Ti, Tc, and LI for 38 patients are shown in Table 2. It can be seen that 20 of 76 examinations during hand grasping and 5 of 67 examinations during tapping exhibited an ipsilateral-dominant βERD pattern. Results from either tasks were then analyzed separately for each hand (supplemental Table II). In 38 grasping examinations with the contralesional hand (or the more severe side for bilateral lesions), an ipsilateral-dominant pattern was observed in 16 of 28 examinations in the AS group, and in 1 of 10 in the NAS group. In grasping with the "other" hand, 25 of 38 examinations were in patients who showed no detectable lesions on the contralateral side, whereas the remaining 13 were with the contralesional hand in patients with bilateral lesions. In this latter set, the ipsilateral pattern was seen in 3 examinations, all of which were in the AS group. Summing up these results, during grasping task, the ipsilateral-dominant βERD pattern was seen in 20 examinations, 19 of which were in patients from the AS group and 1 was in a patient from the NAS group.

Table 3. Incidence of Ipsilateral-Dominant Pattern in Patients With Vascular Disease

	Ipsilateral-Dominant Pattern			
	Hand Grasping		Finger Tapping	
Condition	Present	Absent	Present	Absent
Contralesional hand	19†	32	3	42
Other side hand	1	24	2	20
AS group	19*	37	5	44
NAS group	1	19	0	18

*$P<0.05$ with χ^2 test with Yate correction.

†$P<0.01$ with χ^2 test with Yate correction.

AS group includes patients with atherosclerotic occlusive vascular lesion (n=28); NAS group, patients with nonatherosclerotic occlusive vascular lesion (n=10).

Values represent numbers of examinations. Nine of AS group and 4 of NAS had bilateral lesions, hence the number of examinations with contralesional hand in hand-grasping was 51 (38+13).

In the tapping task, the ipsilateral dominant βERD pattern was observed only in 5 examinations; all were from patients of the AS group (3 were with the "contralesional" and 2 were with the "other" hand).

Table 3 recalculates the results described by taking into consideration the fact that only 25 of 38 patients had no detectable lesion on the side contralateral to the "other" hand, whereas 13 had bilateral lesions. This increased the number of "contralesional hands" to 51. The new calculation shows that in the case of grasping, 19 of 51 examinations with the "contralesional" hand (18 in the AS group and 1 in the NAS group) showed the ipsilateral dominant βERD pattern, whereas the figure was only 1 (a patient in the AS group) of 25 for the other hand. When calculated for each group of patients, 19 of 56 examinations in the AS group (18 with the contralesional and 1 with the "other" hand) and 1 (with the contralesional hand) of 20 examinations in the NAS group exhibited this same pattern. In relation to the self-paced tapping task, the occurrence of an ipsilateral-dominant βERD pattern bore no significant relation to either the hand (contralesional or other) or etiology (AS or NAS group). A representative case that exhibited an ipsilateral-dominant pattern in hand-grasping but not in tapping with contralesional hand is shown (Figure 2).

Factors Related to an Ipsilateral-Dominant βERD Pattern in the Grasping Task With the Hand Contralateral to the Atherosclerotic Occlusive Vascular Lesions

Because the ipsilateral-dominant βERD pattern was observed significantly more frequently in grasping with the contrale-

Table 4. Relationship Between Clinical Factors and the Ipsilateral-Dominant Pattern in 37 Grasping Examinations With the Hand Contralateral to the Site of the Atherosclerotic Occlusive Vascular Lesions

	Ipsilateral-Dominant Pattern in Contralesional Hand Grasping		
Factor	Present	Absent	Significance
Age	70.5 (60–74)	60.5 (55–78)	$P<0.05$*
Tc	13.8 (5.2–25.9)	14.3 (7.0–25.1)	NS
Ti	23.7 (10.4–32.3)	9.9 (3.3–22.6)	$P<0.001$*
Score of sulcal atrophy	4 (2–7)	3 (2–6)	NS
Score of ventricular size	4 (1–7)	3 (1–6)	$P<0.05$*
Score of PVH	5.5 (2–7)	4 (1–7)	$P<0.01$*
Class C in CBF study (+/−)	7/11	6/9	NS
Ischemic event (+/−)	7/11	7/12	NS
Previous infarction (+/−)	3/15	4/15	NS
Side of the hand (left/right)	7/11	7/12	NS
Vascular lesion (MCA/ICA)	7/11	1/18	$P<0.05$†

*With Mann-Whitney *U* test.

†With χ^2 test with Fisher exact probability method.

Number for age was 16 in "present" and 12 in "absent" (28 patients in total). In all other comparisons number was 18 for the former and 19 for the latter, giving a total of 37 examinations. Relevant median values (ranges) are presented: Ti and Tc and peak *t* values on the ipsilateral and contralateral hemisphere, respectively.

sional hand in the AS group, we investigated the effect of several other "factors" on the frequency of this pattern (Table 4) in this same group. In 28 patients, 9 had bilateral lesions, resulting in 37 examinations of contralesional hand-grasping: 18 of these showed the ipsilateral βERD pattern, whereas 19 did not. Statistical analysis shows that the ipsilateral-dominant βERD pattern was seen more often in older patients and was accompanied by a higher Ti, but without a significantly different Tc. Scores for PVH and ventricular size on the side of the vascular lesion had higher values in cases that exhibited the dominant ipsilateral pattern. No significant relation was detected with respect to the incidence of "class C in CBF study," "history of ischemic event," "previous infarction" on the side of the vascular lesion, and the use of "left (nondominant) hand." However, "MCA lesion" as compared with "ICA lesion" showed a significant correlation with the appearance of the ipsilateral-dominant βERD pattern. Individual data of morphological changes in MR images, CBF state, and other "factors" on the vascular lesion side can be found in supplemental Table I.

Discussion

A significant asymmetry in motor-related cortical activity was detected with MEG during grasping with the hand contralateral to the side of an atherosclerotic occlusive vascular disease. The ipsilateral-dominant distribution of βERD was present significantly more frequently in older patients and in those with more severe morphological changes. We feel that this phenomenon, which occurs without any identifiable motor symptoms, is abnormal and reflects subclinical alterations in brain function that accompany atherosclerotic occlusive vascular disease.

Enhanced ipsilateral motor activity has been seen previously during paralytic hand movement in patients with destructive lesions, such as occurring with brain tumor or after stroke, and was initially considered compensatory.[12,17] It has been proposed recently that this activity has a hyperactive component attributable, in some cases, to interhemispheric disinhibition.[18,19] Our results that show characteristic ipsilateral distribution of βERD during grasping with the contralesional hand, a significantly increased activity in the ipsilateral hemisphere without a decrease on the side of the vascular lesion, and a "normal" behavior in the tapping task indicate that hyperactivity on the ipsilateral hemisphere seen in patients with vascular lesions but without motor impairment is not compensatory. These same findings would argue against the possibility that the abnormal ipsilateral motor activity represents an involvement of symmetrical brain areas during the motor task and suggest that the phenomenon originates from other mechanisms.

Similarly to our results, Krakauer et al[20] using functional MRI observed abnormally increased ipsilateral activity during a contralesional hand movement in 6 patients with a unilateral ICA occlusion. The motor tasks they used had observation time windows of 20 seconds for the "active" and "control" states, comparable to those in the hand grasping of our study. However, when we analyzed with MEG during the self-paced tapping task (much shorter, 300-ms periods), we could not detect abnormal ipsilateral activity. This suggests that the different observation time windows record different brain activities.

During a voluntary hand motion, βERD is observed before and during movement execution and is followed by post-movement ERS.[7,21] These frequency changes distribute on the sensorimotor area bilaterally but primarily on the hemisphere contralateral to the examined hand.[7] The postmovement ERS is thought to reflect an inactive, "idling" state and shows an asymmetrical feature considered to be caused by a difference in handedness-related interhemispheric inhibition, "which is more prominent from the dominant than from the

nondominant hemisphere."[21,22] In our study, the "active" time window for hand-grasping was wide enough to encompass the whole of pre-, during-, and postmovement periods; however, that for the tapping task included premovement and motor execution, but less of the postmovement activity. If the postmovement ERS on the ipsilateral hemisphere, which is affected by the inhibition from the contralateral side, is decreased, then it would result in an increase of t value of ERD. Therefore, we propose that when 1 hemisphere activates, the impairment of its inhibitory function induces oscillatory change at the opposite side. For example, when during right hand-grasping in a patient with left ICA stenosis an impairment of the inhibitory function on the left hemisphere fails to deactivate the right hemisphere, this leads to a decrease of ERS on the right hemisphere, and we detect it as the ipsilateral dominant distribution of βERD. A statistically significant relation between the latter and the PVH in the AS group (Table 4) may indicate the contribution of the white matter damage to this phenomenon.

In the present work, we did not measure directly the postmovement ERS because of the difficulty in defining adequately the variation in time periods of post-tap finger movement and the influence of sensory input after the tap. Further studies using different tasks or other methods, such as transcranial magnetic stimulation, to measure cortical inhibitory function are required to confirm or refute our speculation. It should also be mentioned that measurements of motor activity that include pre- and postmovement time periods yield results for "activated areas" that might be strongly influenced by the inhibitory function of the primary activated hemisphere. It would be a great step forward if MEG could be used to evaluate brain activity of duration short enough to be less influenced by inhibitory functions.

Although the abnormal ipsilateral-dominant pattern was seen significantly more often in older patients and in those with higher scores for PVH and ventricular size, it is interesting that the clinically important indications for surgical intervention or stroke prevention, such as "impairment of vasoreactivity," "presence of symptoms," and "presence of an asymptomatic infarction," showed no significant relation. It can be suggested that in addition to CBF impairment caused by occlusive lesions in large vessels, some other factors related to aging and systemic atherosclerosis, which accompany morphological changes such as PVH, may induce subclinical alteration in motor-related cortical activity. A significantly higher incidence of abnormal ipsilateral pattern in patients with MCA lesions might indicate that it reflects functional alterations in particular in this vessel's territory.

In addition to stroke, atherosclerotic occlusive vascular diseases include slow but progressive pathological components that may induce atrophy or white matter change and result in functional impairments, such as vascular dementia. Detection with MEG of ipsilateral hyperactivity, an objective and quantitative measurement independent of CBF or metabolism, could greatly help in early diagnosis and treatment of functional alteration accompanying ischemic cerebrovascular disease.

Summary

We detected abnormal ipsilateral hyperactivity during a contralesional hand-grasping task in patients with atherosclerotic occlusive vascular disease. This phenomenon may represent an impairment of cortical inhibitory function caused by a vascular lesion. Evaluation with MEG could contribute to diagnosis and prevention of functional deteriorations that accompany this class of diseases.

Sources of Funding

This work was supported by grant-in-aid for scientific research (19790995) from the Japanese Ministry of Education, Science and Culture, by a grant from National Cardiovascular Research Institute (J040701213, J050701211), and by a grant from Public Health Research Foundation (Tokyo, Japan).

Disclosures

None.

References

1. North American Symptomatic Carotid Endarterectomy Trial Collaborators. Beneficial effect of carotid endarterectomy in symptomatic patients with high-grade carotid stenosis. *N Engl J Med*. 1991;325:445–453.
2. Kern R, Steinke W, Daffertshofer M, Prager R, Hennerici M. Stroke recurrences in patients with symptomatic vs asymptomatic middle cerebral artery disease. *Neurology*. 2005;65:859–864.
3. Mathiesen EB, Waterloo K, Joakimsen O, Bakke SJ, Jacobsen EA, Bonaa KH. Reduced neuropsychological test performance in asymptomatic carotid stenosis: The Tromso study. *Neurology*. 2004;62:695–701.
4. Chatrian GE, Petersen MC, Lazarte JA. The blocking of the rolandic wicket rhythm and some central changes related to movement. *Electroencephalogr Clin Neurophysiol*. 1959;11:497–510.
5. Pfurtscheller G. Graphical display and statistical evaluation of event-related desynchronization (ERD). *Electroencephalogr Clin Neurophysiol*. 1977;43:757–760.
6. Neuper C, Pfurtscheller G. Event-related dynamics of cortical rhythms: Frequency-specific features and functional correlates. *Int J Psychophysiol*. 2001;43:41–58.
7. Pfurtscheller G. Central beta rhythm during sensorimotor activities in man. *Electroencephalogr Clin Neurophysiol*. 1981;51:253–264.
8. Crone NE, Miglioretti DL, Gordon B, Lesser RP. Functional mapping of human sensorimotor cortex with electrocorticographic spectral analysis. Ii. Event-related synchronization in the gamma band. *Brain*. 1998;121:2301–2315.
9. Oshino S, Kato A, Wakayama A, Taniguchi M, Hirata M, Yoshimine T. Magnetoencephalographic analysis of cortical oscillatory activity in patients with brain tumors: Synthetic aperture magnetometry (SAM) functional imaging of delta band activity. *Neuroimage*. 2007;34:957–964.
10. Robinşon SE, Vrba J. Functional neuroimaging by synthetic aperture magnetometry (SAM). *Recent Advances in Biomagnetism*. Sendai, Tohoku University Press;1999:302–305.
11. Taniguchi M, Kato A, Fujita N, Hirata M, Tanaka H, Kihara T, Ninomiya H, Hirabuki N, Nakamura H, Robinson SE, Cheyne D, Yoshimine T. Movement-related desynchronization of the cerebral cortex studied with spatially filtered magnetoencephalography. *Neuroimage*. 2000;12:298–306.
12. Taniguchi M, Kato A, Ninomiya H, Hirata M, Cheyne D, Robinson SE, Maruno M, Saitoh Y, Kishima H, Yoshimine T. Cerebral motor control in patients with gliomas around the central sulcus studied with spatially filtered magnetoencephalography. *J Neurol Neurosurg Psychiatry*. 2004;75:466–471.
13. Hirata M, Kato A, Taniguchi M, Saitoh Y, Ninomiya H, Ihara A, Kishima H, Oshino S, Baba T, Yorifuji S, Yoshimine T. Determination of language dominance with synthetic aperture magnetometry: Comparison with the Wada test. *Neuroimage*. 2004;23:46–53.

14. Oldfield RC. The assessment and analysis of handedness: The Edinburgh inventory. *Neuropsychologia*. 1971;9:97–113.
15. Manolio TA, Kronmal RA, Burke GL, Poirier V, O'Leary DH, Gardin JM, Fried LP, Steinberg EP, Bryan RN. Magnetic resonance abnormalities and cardiovascular disease in older adults. The cardiovascular health study. *Stroke*. 1994;25:318–327.
16. Imaizumi M, Kitagawa K, Hashikawa K, Oku N, Teratani T, Takasawa M, Yoshikawa T, Rishu P, Ohtsuki T, Hori M, Matsumoto M, Nishimura T. Detection of misery perfusion with split-dose ^{123}I-iodoamphetamine single-photon emission computed tomography in patients with carotid occlusive diseases. *Stroke*. 2002;33:2217–2223.
17. Johansen-Berg H, Rushworth MF, Bogdanovic MD, Kischka U, Wimalaratna S, Matthews PM. The role of ipsilateral premotor cortex in hand movement after stroke. *Proc Natl Acad Sci U S A*. 2002;99:14518–14523.
18. Shimizu T, Hosaki A, Hino T, Sato M, Komori T, Hirai S, Rossini PM. Motor cortical disinhibition in the unaffected hemisphere after unilateral cortical stroke. *Brain*. 2002;125:1896–1907.
19. Murase N, Duque J, Mazzocchio R, Cohen LG. Influence of interhemispheric interactions on motor function in chronic stroke. *Ann Neurol*. 2004;55:400–409.
20. Krakauer JW, Radoeva PD, Zarahn E, Wydra J, Lazar RM, Hirsch J, Marshall RS. Hypoperfusion without stroke alters motor activation in the opposite hemisphere. *Ann Neurol*. 2004;56:796–802.
21. Pfurtscheller G, Stancak A Jr, Neuper C. Post-movement beta synchronization. A correlate of an idling motor area? *Electroencephalogr Clin Neurophysiol*. 1996;98:281–293.
22. Stancak A Jr, Pfurtscheller G. Event-related desynchronisation of central beta-rhythms during brisk and slow self-paced finger movements of dominant and nondominant hand. *Brain Res Cogn Brain Res*. 1996;4:171–183.